

Field Emission of Carbon Nanotubes Grown on Silicon Nanowires Using Thermal Chemical Vapor Deposition

SHIH-FONG LEE¹, LI-YING LEE^{1,2} and YUNG-PING CHANG¹

¹*Department of Electrical Engineering, Da-Yeh University*

No. 168, University Rd., Da-Tsuen, Changhua, Taiwan 51591, R.O.C.

²*Department of Electronic Engineering, Chung Chou Institute of Technology*

No. 6, Lane 2, Sec. 3, Shanjiao Rd., Yuanlin, Changhua, Taiwan 51003, R.O.C.

ABSTRACT

In this study, carbon nanotubes (CNTs) were synthesized on Si nanowires (SiNWs) using thermal chemical vapor deposition. SiNWs were directly synthesized onto Si substrates through a solid-liquid-solid (SLS) phase growth mechanism at elevated temperatures. The growth temperature for CNT was 900 °C at an ambient pressure. Methane and argon gases were used for CNT synthesis. In this study, scanning electron microscopy (SEM) and transmission electron microscopy (TEM) images were used to observe the surface morphology and sidewall structure, and Raman spectroscopy was employed to investigate the structure of CNTs. The carbon nanotubes grown on SiNWs demonstrated a multiwalled structure with defective graphite sheets in the wall. Raman spectra determined the SiNW carbon nanotubes had poor crystallinity, or more amorphous carbon, than those grown on plain Si substrate. Compared with CNTs grown on flat silicon substrates, CNTs grown on SiNWs exhibit superior field emission characteristics. The Fowler-Nordheim plot displayed a good linear fit, indicating the emission current of carbon nanotubes follows a Fowler-Nordheim behavior.

Key Words: carbon nanotubes (CNTs), field emission, thermal chemical vapor deposition (thermal CVD), silicon nanowires (SiNWs)

藉由熱化學氣相沉積在矽奈米絲上成長奈米碳管及其場發射

李世鴻¹ 李麗英^{1,2} 張永平¹

¹大葉大學電機工程系

51591 彰化縣大村鄉學府路 168 號

²中州技術學院電子系

510 彰化縣員林鎮山腳路三段 2 巷 6 號

摘 要

本研究以熱化學氣相沉積法在矽奈米絲上成長奈米碳管。矽奈米絲的製備則是使用一種固相-液相-固相 (solid-liquid-solid, SLS) 機制, 直接從矽基板藉由加熱來成長。甲烷與氫氣被用來正常氣壓、900°C 溫度下成長奈米碳管。本研究使用電子顯微鏡 (scanning electron microscope, SEM) 與穿透式電子顯微鏡 (transmission electron microscopy, TEM) 來觀察奈米碳管的表面形

態，使用拉曼光譜 (RAMAN) 分析奈米碳管的結構性質。從 SEM 及 TEM 的研究結果清楚顯示，在矽奈米絲上成長的奈米碳管呈現多壁結構狀態，且奈米碳管管壁上存在有許多缺陷狀態及許多石墨奈米顆粒。從拉曼光譜數據可以發現，在矽奈米絲上所成長的奈米碳管，比在平面矽基板上成長的奈米碳管有較大的結晶缺陷與較多的非晶質碳存在。電性量測結果則呈現出在矽奈米絲上成長的奈米碳管會有較佳的場發射結果，且符合 Fowler-Nordheim 場發射特徵。

關鍵詞：奈米碳管，場發射，熱化學氣相沉積，矽奈米絲

I. INTRODUCTION

Since the first observation of carbon nanotubes (CNTs) [15], extensive research has been done on the synthesizing methods: arc discharge [2, 16], laser vaporization [33], pyrolysis [32], and plasma-enhanced or thermal chemical vapor deposition (CVD) [8, 17, 21, 24, 29, 31]. Among these synthesis methods, CVD has many advantages such as high purity, high yield, simple process, selective growth, vertical alignment, and large area uniformity.

Both CNT and silicon nanowires (SiNW) are promising nanomaterials as building blocks of future nanodevices owing to their dimensions and electronic properties. One of the motivations of using CNTs or SiNWs for field emission is the large geometric field enhancement factor, which can provide lower turn-on voltages [3, 25]. It has been reported that CNTs grown on SiNWs may have distinctive properties [5]. The reason for using the composite structure lies in the fact that higher CNT density and reduced screening effects can be obtained from this tree-like three-dimensional structure. According to Fu [10] and Chhowalla [7], the CNT/SiNW structure could be favorable for field emission applications. The good field emission performance is attributed to the morphology of CNT/SiNW, especially the formation of a sharp and vertically aligned CNT array. The CNT/SiNW might be an ideal candidate cathode for potential applications in flat panel displays, which need a low-power, low-temperature, and high-current electron emitter. However, systematic studies on the surface morphology and field-emission characteristics of CNTs grown on SiNWs by thermal CVD are still very rare.

In synthesizing CNT, the catalysts are coated on the substrates prior to CNT growth. Catalysts such as Fe, Co, Ni or other transition metals and alloys are normally used for CNT growth by decomposing hydrocarbon sources. CNT can be grown on most substrates such as silicon, silica, alumina or aluminosilicate, as long as the temperature is sustained in growth [6, 8]. There are a few reports discussing CNT synthesized on different substrate materials. Two problems arise in CNT growth on substrates are that transition metals are easily diffused into the carbon substrates and that different phases of carbon materials are able to form on the substrates

[19, 35]. The field emission properties of CNTs grown on various substrates have been reported, such as silicon substrates [3], porous silicon substrates [9], metal substrates and plastic substrates [13, 34]. But all the substrates mentioned above are flat, and there are few reports on the synthesis and field emission properties of CNTs grown on non-flat and geometry controllable substrates. Here we report another structure of the emitters by synthesizing carbon nanotubes on silicon nanowires (SiNWs), the field emission properties of which are presented.

In this study, we synthesized multi-walled CNTs directly on SiNWs using thermal chemical vapor deposition. We also investigated the structure of CNTs synthesized on SiNWs and Si wafer using scanning electron microscopy (SEM), transmission electron microscopy (TEM), electron dispersive spectrometer (EDS) and Raman spectroscopy. Field emission from the as-grown CNTs was also examined.

II. EXPERIMENTAL DETAILS

In this work, thermal CVD was utilized to synthesize SiNWs and CNTs. The flowchart for growth and measurement steps is illustrated in Fig. 1. In this work, SiNWs were synthesized on n-type Si (100) substrate through a solid-liquid-solid (SLS) phase growth mechanism [27]. The synthesis of SiNWs was carried out in a high-temperature tube furnace. Si wafers (100) were cleaned by the standard clean process. The cleaned wafer surface was then deposited with Ni film (5-20 nm of thickness) using an ultrahigh vacuum thermal evaporator at room temperature. The wafer coated with Ni film was placed on a ceramic boat, and placed into the center of the tube-furnace for further heating at 1000°C in an Ar atmosphere for 2 hr. The metal catalyst of nickel film induced the growth of SiNWs.

In this study, the growth of CNTs was performed using a thermal CVD system already described in Lee [22-23]. SiNWs and silicon wafer substrates were cleaned with standard RCA procedure. Ni film was subsequently evaporated onto the silicon substrate as the catalyst metal [18]. The thickness of Ni was 7.5 nm which was precisely controlled with a thickness monitor. Substrates with Ni were mounted on a ceramic holder. The specimen was placed into the quartz reactor and the

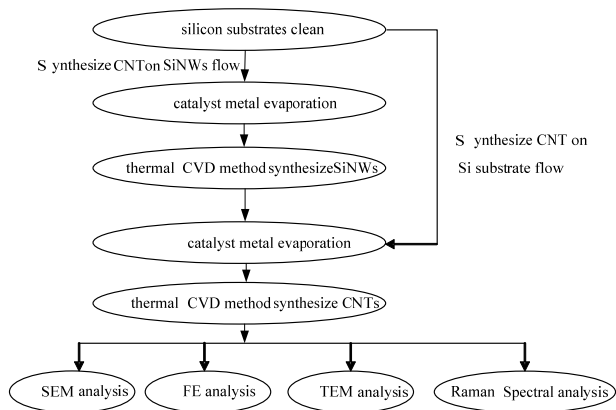


Fig. 1. Flow chart for the synthesis and characterization of CNTs on SiNW and Si substrates.

chamber was pumped down to less than 10^{-3} Torr using a mechanical pump. Before reaching the growth temperature at 900°C , Ar (1800 sccm) was fed into reactor and temperature was gradually increased until it reached target temperature (900°C) and maintained at that temperature for 10 min for it to stabilize. The temperature and pressure for synthesis were about 900°C and 1 atm, respectively. After temperature and pressure were stabilized, CH_4 was introduced at a flow rate of 100 sccm. The growth time was 15 min. The samples were then cooled in an Ar flow ambient.

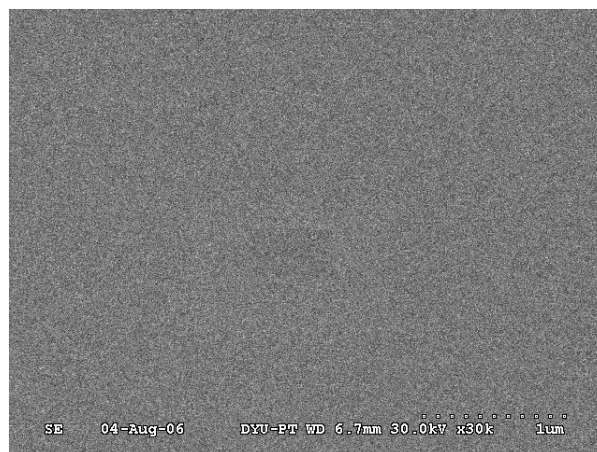
Surface morphology and structural properties for the synthesized CNTs after acid solution post-treatments were characterized with SEM, TEM and Raman spectroscopy. A Hitachi S-3000N was used to obtain SEM image, a Philips EM-430ST electron microscope operated at 200 kV was used to obtain TEM images, and a 3-D nanometer scale Raman PL microspectrometer whose excitation is a 632.8 nm He-Ne laser was used to obtain Raman spectra of the CNTs.

The field emission measurements were carried out in high vacuum to ensure accurate measurement results. Synthesized CNTs were pasted with silver paste or carbon paste onto a glass substrate coated with conducting indium tin oxide (ITO) and dried in an oven. The glass substrate together with CNTs was mounted on a test fixture as the cathode, while an ITO glass substrate was used as the anode. The emission area, which is the area of sample exposed for electron emission, is $\sim 0.007\text{ cm}^2$. The spacing between two electrodes was adjusted to $110\text{ }\mu\text{m}$. To ensure accurate measurement on the emitted currents of CNTs, the measurement was carried out in high vacuum. Our previous measurement results revealed that measurement carried out at a pressure of less than 10^{-3} Torr had very little effect on the measured emitted current. In this study, the vacuum chamber was pumped down to 10^{-2} Torr with a mechanical pump, and subsequently pumped down to 10^{-5} Torr

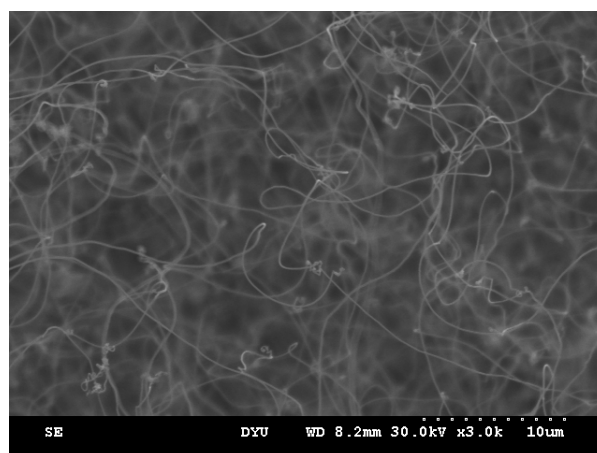
with a turbomolecular pump. A Keithley 237 high-voltage source-measure unit was used to apply voltage (up to 1000V) and to measure the emitted current with pA sensitivity, allowing for the accurate characterization of current-voltage (I - V) behavior. The Keithley 237 source-measure unit was fully automated with a computer.

III. RESULTS AND DISCUSSIONS

A detailed view of the surface morphology has been obtained using the scanning electron microscope (SEM). Fig. 2(a) shows the SEM images of the silicon wafer. The surface of the film was observed to be smooth and tidy. Fig. 2(b) shows the typical SEM images of SiNWs that were grown on n-type Si (100) substrate through a solid-liquid-solid (SLS) phase growth mechanism. It can be found from Fig. 2(b) that randomly oriented silicon nanowires have grown all over the substrates and the average diameter of the synthesized silicon nanowires is 92 nm.



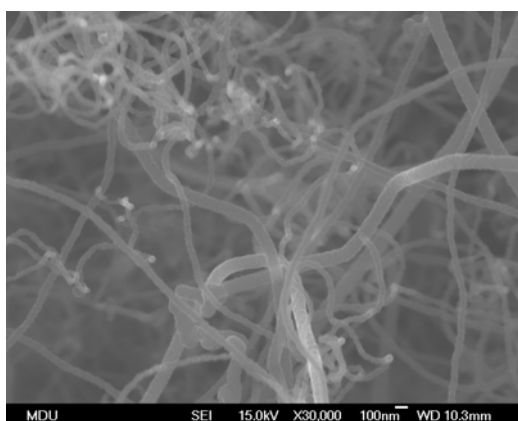
(a) SEM images of the morphology of silicon wafer



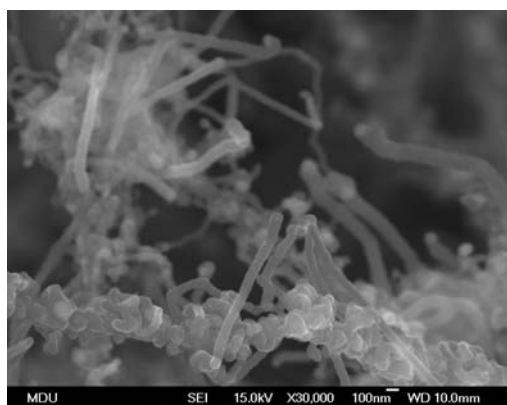
(b) SEM images of silicon nanowires

Fig. 2. The SEM images of silicon wafer and silicon nanowires.

Figs. 3(a) and (b) show the SEM images of the CNTs films which were grown on silicon wafer and SiNWs thin films, respectively. As can be clearly seen in Fig. 3(a), there is almost no amorphous carbon present on the surface of the substrate for the synthesized CNTs grown on silicon wafer. The outer diameter of the tubes ranged in 50-90 nm and the typical length of tubes was about 1-5 μm . The CNT surfaces were smooth and tidy. It can also be found that randomly oriented CNTs have grown all over the substrates for the CNTs grown on silicon substrate. However, the configuration of nanotubes in the top layer of film was entirely different for the CNTs grown on SiNWS. The surfaces of CNTs became rough (Fig. 3(b)) and were covered by ball nano-nodes. Many nano-scale particles along the tubes appeared just like nodes and the spaces between tubes were enlarged. The surfaces of nodes are highly curved and have a high density of structure defects. Both the experiments [30] and theoretical studies [4] have shown that the electronic and geometrical structures of the tips and the defects in the CNTs have predominant effects on the field emission characteristics of the CNTs.



(a) Top-view SEM images of the CNTs grown on silicon substrate



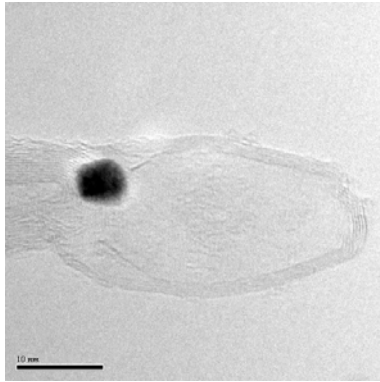
(b) Top-view SEM images of the CNTs grown on silicon nanowires

Fig. 3. The SEM images of the CNTs films which were grown on silicon wafer and SiNWs thin films.

TEM investigations were carried out to study the microstructure of nanotubes in detail. Fig. 4(a) is the TEM microstructure of the CNTs depicted in Fig. 3(a), showing that the CNTs consist of hollow compartments. It also reveals closed tips with encapsulated catalytic particles and the compartment layers with a curvature toward the tip. The encapsulation of catalytic particle at the tip suggests that the growth of bamboo-shaped CNTs using our thermal CVD method follows the tip growth mechanism. Fig. 4(b) and 4(c) are the TEM microstructure of the CNTs depicted in Fig. 3(b). It is clear from Fig. 4(b) and 4(c) that the nano-particles are multi-shell ball-like nodes with a central cavity and some nanotube graphite layers were bent or wavy. The surfaces of nodes are highly curved and have high density of structure defects. These changes indicated that there were many defects and dangling bonds on the surface of the tubes. The image of the bent nanotube graphite layers and nanoparticles would contribute to electron emission.

Fig. 5 shows the Raman spectra of the samples grown on silicon substrate and SiNWs thin films, respectively. All spectra are dominated by two intensity peaks located at 1328 cm^{-1} (D Line) and 1588 cm^{-1} (G line) confirming the multi-wall nature of the CNTs. The D line is generally attributed to defects in the curved graphite sheet, sp^3 carbon or other impurities [1]. The G line corresponds to the movement in opposite direction of two neighboring carbon atoms in a graphitic sheet and it indicates the presence of crystalline graphitic carbon in the CNT film [26]. The ratio of the intensities between D peak and G peak I_D/I_G is an indication of the amount of disorder in the nanotube materials, allowing us to estimate the crystallite size and relative extent of structural defects. As shown in Fig. 5, the calculated I_D/I_G ratios are 1.02 and 1.12 for the samples grown on silicon substrate and SiNW thin films, respectively. The I_D/I_G ratios of the CNTs grown on SiNWs thin films is bigger than those of the CNTs grown on silicon substrate that indicated the increasing of the defects and nano-nodes more specifically. From Fig. 5, the appearance of the relatively strong D peaks in CNT films grown on SiNWs can possibly result from the existence of nano-nodes and the structural defects in the nanotubes graphite sheets. These nano-nodes and defects provide more emission sites on the nanotubes surface.

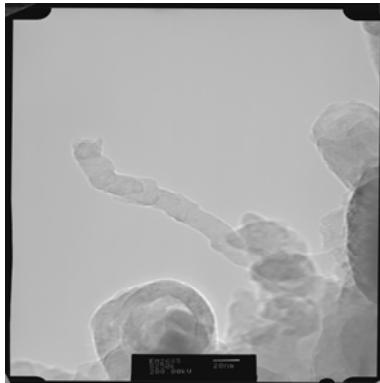
Field emission is one of the most promising applications for carbon nanotubes. Fig. 6 illustrates the typical curves of electron emission current density versus electric field from CNT emitter grown on silicon substrate and SiNWs thin films, respectively. It is evident that the CNT films grown on SiNWs thin film exhibit better field emission properties. In Fig. 6, the turn-on electric fields, defined as the fields to obtain a current



(a) Top-view TEM images of the CNTs grown on silicon substrate



(b) Top-view TEM images of the CNTs grown on silicon nanowires



(c) Top-view TEM images of the CNTs grown on silicon nanowires

Fig. 4. The TEM images of the CNTs grown on silicon substrate and SiNWs thin film.

density of $0.1 \mu\text{A}/\text{cm}^2$, are $2.8 \text{ V}/\mu\text{m}$ and $1.1 \text{ V}/\mu\text{m}$ for the samples synthesized on silicon substrate and SiNWs thin films, respectively. Furthermore, a current density of $1 \text{ mA}/\text{cm}^2$ required basically for flat panel display is obtained at $9.0 \text{ V}/\mu\text{m}$ and $6.2 \text{ V}/\mu\text{m}$ for the samples synthesized with silicon substrate and SiNWs thin films, respectively. We see that the CNT synthesized on SiNWs thin films have a lower threshold field than the CNT synthesized on silicon substrate.

The field enhancement factor can be calculated with the Fowler-Nordheim equation. This model describes the electron

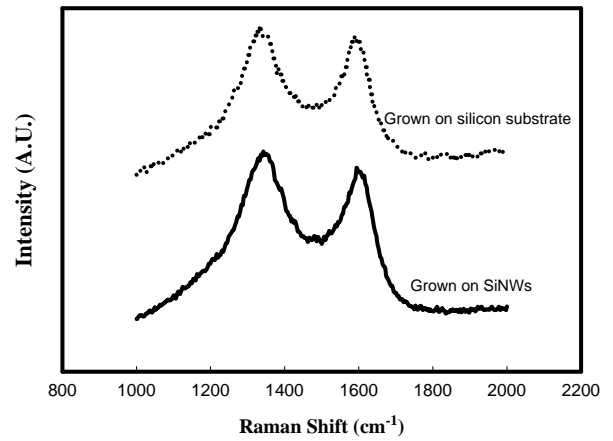


Fig. 5. Raman spectra of carbon nanotubes grown on silicon substrate and silicon nanowires.

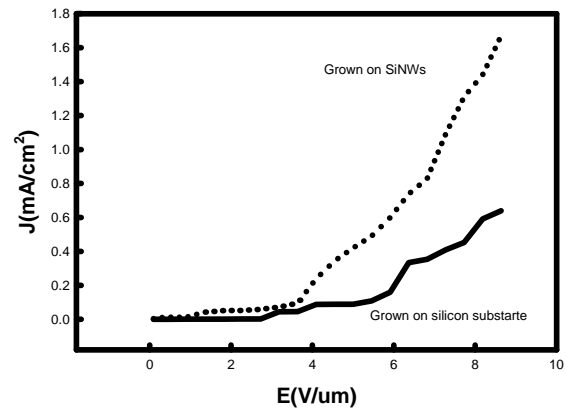


Fig. 6. Comparison of the emission characteristics for the CNTs grown on silicon substrate and silicon nanowires.

emission from a flat surface by tunneling through a triangular surface potential barrier. The emitted current I is proportional to $F^2 \exp(-\beta\Phi^{3/2}/F)$, where F is the applied field just above the emitting surface, Φ is the work function, and B is a constant ($B = 6.83 \times 10^{-9} \text{ VeV}^{3/2} \text{ m}^{-1}$) [11]. Generally speaking, F is not known exactly and is therefore taken here as $F = \beta E = \beta V/d$, with the applied voltage V , the inter-electrode distance d , and the macroscopic applied field $E = V/d$. The proportionality constant β is called the field enhancement factor to account for the local enhancement of electric field caused by non-flat surface. The work function was assumed to be equal to 5 eV , which is a reasonable assumption for carbon based field emitters [20]. Fig. 7 shows the corresponding Fowler-Nordheim (F-N) plots for the emission characteristics shown in Fig. 6 at high fields. In Fig. 7, these approximately straight lines indicate that the emitted electrons are indeed dominated by field emission. It is seen from Fig. 7 that the

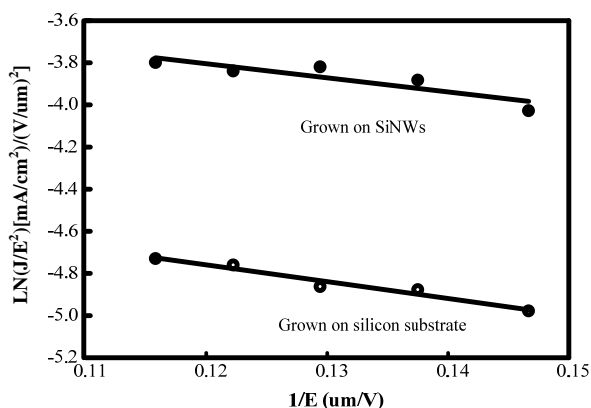


Fig. 7. Corresponding Fowler-Nordheim plots for the emission characteristics shown in Fig. 6.

slope of the F-N plots decreases for CNTs grown on SiNWs thin films. The slope values are 8.05 and 7.4 for the samples grown on silicon substrate and SiNWs thin films, respectively. The decrease in the slope means a decrease in the average work function of CNT emitters and/or an increase in the field enhancement factor corresponding to the sharpening of emitter.

Therefore, we believe that the low turn-on field and high emission current density of CNTs grown on SiNWs thin films are obtained for two reasons: (1) The geometrical enhancement effect was introduced by the particles in the nano-nodes. The CNTs grown on SiNW thin films produce nanoparticles as the emitters on the CNTs wall, and the curvature radii of these nanoparticle emission sites are much smaller. Thus, the field enhancement factor β is increased. The large increase in the emission current is due to the high field concentration at the nano-nodes. Besides of the electronic structure, geometrical effects also affect the field emission. Zhou and his coworker's calculation indicated [36] that the field enhancement factor of the tip is approximately 125 times that of the nanotube body. In our study, the node has a similar structure to the tip of the CNTs as shown in Figs. 3 and 4. Therefore, the electrons emitted from the nodes should be much more than those from the original tube. Evidently, the changing in the geometrical structure of the CNTs could enhance the field emission property drastically. (2) The other reason is the decrease in the effective work function on emitter surface. We attributed the enhancement of emission properties observed in our experiments to the carbon nano-nodes formed due to bending of graphene sheets along the CNT wall. It should be noted that the graphene sheet arc structure appearance is usual for various graphite materials [14]. These arc graphene sheets may be considered as sp^3 -like defects in the sp^2 -like graphite network [12]. The electron states density of the sp^3 -like clusters is higher than that of the sp^2 -like graphite part, providing a

reduction of the potential barrier width for electrons escaping into vacuum [28]. SEM and TEM images give a direct evidence of the presence of defects along the nanotubes body. In addition, the Raman spectra demonstrate that the CNTs have some tetrahedral structure characteristics which play an important role for the enhancement of field emission. All of these characteristics are beneficial to electron field emission. In this study, the CNT grown on SiNWs thin films corresponds to depositing a sp^3 -rich surface layer of the nano-node nanoparticles with low work functions onto the carbon nanotube film, which favorably improve the emission characteristics of the films.

IV. CONCLUSIONS

The purpose of this work is to investigate the structural and electronic properties of CNTs grown on SiNWs thin films and to study how the SiNWs thin films can affect the surface morphology of the synthesized CNTs in order to provide an effective method to enhance the field emission characteristics of the CNTs. In this study, the effects of SiNWs thin films on the electronic properties and field emission were investigated. The surface morphology and microstructural characteristics of CNT films were examined by SEM, TEM and Raman spectroscopy. The change in the electronic properties of the CNTs grown on SiNWs thin films is due to the CNT surface structure. The improvement in field emission is mainly resulted from the increase in the number of emitting sites, the sharpening of the emitter, and the presence of nano-nodes and defect on the surface of CNTs. Our experimental results clearly demonstrate that the CNTs grown on SiNWs thin films exhibit good field emission properties, low turn-on emission field and high emission current density.

V. ACKNOWLEDGEMENT

This work was supported in part by National Science Council of R.O.C. under contract NSC-99-2221-E-212-024-MY2.

REFERENCES

1. Bacsa, W. S., D. Ugarte, A. Chatelain and W. A. De Heer (1994) High resolution electron microscope and inelastic light scattering of purified multishelled carbon nanotubes. *Physical Review B*, 50, 15473-15476.
2. Bethune, D. S., C. H. Kiang, M. S. de Vries, G. Gorman, R. Savoy, J. Vazquez and R. Beyers (1993) Cobalt-catalysed growth of carbon nanotubes with single-atomic-layer walls. *Nature*, 363, 605-607.
3. Bonard, J. M., M. Croci, C. Klinke, R. Kurt, O. Noury and

- N. Weiss (2002) Carbon nanotube films as electron field emitters. *Carbon*, 40, 1715-1728.
4. Carroll, D. L., P. Redlich, P. M. Ajayan, J. C. Charlier, X. Blase, A. De Vita and R. Car (1997) Electronic structure and localized states at carbon nanotube tips. *Physical Review Letters*, 78, 2811-2815.
 5. Chang, C. S., S. Chattopadhyay, L. C. Chen, K. H. Chen, C. W. Chen and Y. F. Chen (2003) Band gap dependence of field emission from one dimensional nanostructures grown on n-type and p-type silicon substrates. *Physical Review B*, 68, 125322-1-125322-5.
 6. Cheng, H. M., F. Li, G. Su, H. Pan and M. Dresselhaus (1998) Large-scale and low cost synthesis of single wall carbon nanotubes by the catalyst pyrolysis of hydrocarbons. *Applied Physics Letters*, 72, 3283-3284.
 7. Chhowalla, M., C. Ducati, N. L. Rupesinghe, K. B. K. Teo and G. A. J. Amaratunga (2001) Field emission from short and stubby vertically aligned carbon nanotubes. *Applied Physics Letters*, 79, 2079-2081.
 8. Fan, S. S., M. G. Chapline, N. R. Franklin, T. W. Tombler, A. M. Cassell and H. J. Dai (1999) Self-oriented regular arrays of carbon nanotubes and their field emission properties. *Science*, 283, 512-514.
 9. Fan, S., W. Liang, H. Dang, N. Franklin, T. Tombler, M. Chapline and H. Dai (2000) Carbon nanotube arrays on silicon substrates. *Physica E*, 8, 179-183.
 10. Fu, Y. Q., A. Colli, A. Fasoli, J. K. Luo, A. J. Flewitt, A. C. Ferrari and W. I. Milne (2009) Deep reactive ion etching as a tool for nanostructure fabrication. *Journal of Vacuum Science and Technology B*, 27, 1520-1526.
 11. Gadzuk, J. W. and E. W. Plummer (1973) Field emission energy distribution[s] (FEED). *Reviews of Modern Physics*, 45, 487-548.
 12. Hiura, H., T. W. Ebbesen, J. Fujita, K. Tanigaki and T. Takada (1994) Role of sp^3 defect structures in graphite and carbon nanotubes. *Nature*, 367, 148-151.
 13. Hofmann, S., C. Ducati, B. Kleinsorge and J. Robertson (2003) Direct growth of aligned carbon nanotube field emitter arrays onto plastic substrates. *Applied Physics Letters*, 83, 4661-4663.
 14. Huang, J. Y., H. Yasuda and H. Mori (1999) Highly curved carbon nanostructures produced by ball-milling. *Chemical Physics Letters*, 303, 130-134.
 15. Iijima, S. (1991) Helical microtubules of graphitic carbon. *Nature*, 354, 56-58.
 16. Iijima, S. and T. Ichihashi (1993) Single-shell carbon nanotubes of 1-nm diameter. *Nature*, 363, 603-605.
 17. Journet, C., W. K. Maser, P. Bernier, A. Loiseau, M. Lamy de la Chapelle, S. Lefrant, P. Deniard, R. Lee, and J. E. Fischer (1997) Large-scale production of single-walled carbon nanotubes by the electric-arc technique. *Nature*, 388, 756-758.
 18. Kichambare, P. D., D. Qian, E. C. Dickey and C. A. Grimes (2002) Thin film metallic catalyst coatings for the growth of multiwalled carbon nanotubes by pyrolysis of xylene. *Carbon*, 40, 1903-1909.
 19. Kung, S. C., K. C. Hwang and I. N. Lin (2002) Oxygen and ozone oxidation-enhanced field emission of carbon nanotubes. *Applied Physics Letters*, 80, 4819-4821.
 20. Küttel, O. M., O. Gröning, Ch. Emmenegger, L. Nilsson, E. Maillard, L. Diederich and L. Schlapbach (1999) Field emission from diamond, diamond-like and nanostructured carbon films. *Carbon*, 37, 745-752.
 21. Lee, C. J., D. W. Kim, T. J. Lee, Y. C. Choi, Y. S. Park, W. S. Kim, Y. H. Lee, W. B. Choi, N. S. Lee, J. M. Kim, Y. G. Choi and S. C. Yu (1999) Synthesis of uniformly distributed carbon nanotubes on a large area of Si substrates by thermal chemical vapor deposition. *Applied Physics Letters*, 75, 1721-1723.
 22. Lee, S. F., Y. P. Chang and L. Y. Lee (2008) Effects of annealing Ni catalyst in nitrogen-based gases on the surface morphology and field-emission properties of thermal chemical vapor deposited carbon nanotubes. *New Carbon Materials*, 23, 302-308.
 23. Lee, S. F., Y. P. Chang and L. Y. Lee (2009) Plasma treatment effects on surface morphology and field emission characteristics of carbon nanotubes. *Journal of Materials Science: Materials in Electronics*, 20, 851-857.
 24. Li, W. Z., S. S. Xie, L. X. Qian, B. H. Chang, B. S. Zou, W. Y. Zhou, R. A. Zhao and G. Wang (1996) Large-scale synthesis of aligned carbon nanotubes. *Science*, 274, 1701-1703.
 25. Milne, W. I., K. B. K. Teo, G. A. J. Amaratunga, P. Legagneux, L. Gangloff, J. P. Schnell, V. Semet, V. Thien Binh and O. Groening (2004) Carbon nanotubes as field emission sources. *Journal of Materials Chemistry*, 14, 933-943.
 26. Nemanich, R. J. and S. A. Solin (1979) First- and second-order Raman scattering from finite-size crystals of graphite. *Physical Review B*, 20, 392-401.
 27. Nilsson, L., O. Groening, C. Emmenegger, O. Kuettel, E. Schaller, L. Schlapbach, H. Kind, J-M. Bonard and K. Kern (2000) Scanning field emission from patterned carbon nanotube films. *Applied Physics Letters*, 76, 2071-2073.
 28. Obratsov, A. N., I. Pavlovsky, A. P. Volkov, E. D.

- Obraztsova, A. L. Chuvilin and V. L. Kuznetsov (2000) Aligned carbon nanotube films for cold cathode application. *Journal of Vacuum Science and Technology B*, 18, 1059-1063.
29. Ren, Z. F., Z. P. Huang, J. W. Xu, J. H. Wang, P. Bush, M. P. Siegal and P. N. Provencio (1998) Synthesis of large arrays of well-aligned carbon nanotubes on glass. *Science*, 282, 1105-1107.
30. Rinzler, A. G., J. H. Hafner, P. Nikolaev, L. Lou, S. G. Kim, D. Tomanek, P. Nordlander, D. T. Colbert and R. E. Smalley (1995) Unraveling nanotubes: Field emission from an atomic wire. *Science*, 269, 1550-1553.
31. Sung, S. L., S. H. Tsai, C. H. Tseng, F. K. Chiang, X. W. Liu and H. C. Shih (1999) Well-aligned carbon nitride nanotubes synthesized in alumina by electron cyclotron resonance chemical vapor deposition. *Applied Physics Letters*, 74, 197-199.
32. Terrones, M., N. Grobert, J. Olivares, J. P. Zhang, H. Terrones, K. Kordatos, W. K. Hsu, J. P. Hare, P. D. Townsend, K. Prassides, A. K. Cheetham, H. W. Kroto and D. R. M. Walton (1997) Controlled production of aligned –nanotube bundles. *Nature*, 388, 52-55.
33. Thess, A., R. Lee, P. Nikolaev, H. Dai, P. Petit, J. Robert, C. Xu, Y. H. Lee, S. G. Kim, A. G. Rinzler, D. T. Colbert, G. Scuseria, D. Tománek, J. E. Fischer and R. E. Smalley (1996) Crystalline ropes of metallic carbon nanotubes. *Science*, 273, 483-487.
34. Yamamoto, A. and T. Tsutsumoto (2003) Field emission from carbon films deposited on steel substrate. *Diamond and Related Materials*, 12, 1729-1734.
35. Zhang, J., T. Feng, W. Yu, X. Liu, X. Wang and Q. Li (2004) Enhancement of field emission from hydrogen plasma processed carbon nanotubes. *Diamond and Related Materials*, 13, 54-59.
36. Zhou, G., W. Duan and B. Gu (2001) Dimensional effects on field emission properties of the body for single-walled carbon nanotube. *Applied Physics Letters*, 79, 836-838.

Received: Oct. 11, 2010 Revised: Dec. 22, 2010

Accepted: May 04, 2011